Green Chemistry

PAPER

View Article Online
View Journal | View Issue

Cite this: *Green Chem.*, 2022, **24**, 3152

Recovery of low molecular weight compounds from alkaline pretreatment liquor *via* membrane separations†

Patrick O. Saboe, [a] Emily G. Tomashek, [a]‡ Hanna R. Monroe,§[a] Stefan J. Haugen, [a] Ryan L. Prestangen,¶[a] Nick S. Cleveland,[a] Renee M. Happs, [a] Joel Miscall,[a] Kelsey J. Ramirez, [a] Rui Katahira, [a] Eric C. D. Tan, [a] Jipeng Yan,[b] Ning Sun, [b] Gregg T. Beckham [a] and Eric M. Karp *[a]

Lignin is an abundant renewable resource that is a promising substrate for upgrading to fuels and chemicals. However, lignin-rich biorefinery streams are often physically and chemically complex, and could benefit substantially from fractionation. In this work, a membrane process was developed to fractionate low molecular weight (LMW) lignin-related compounds (molecular weight (MW) < 1000 Da) from a lignin-rich, alkaline pretreated liquor (APL) prepared from pretreatment of corn stover with NaOH. The developed membrane process exhibits up to 98.5% rejection of high molecular weight (HMW) (MW > 1000 Da) species and generates a permeate stream with >80% recovery of LMW lignin-related compounds including aromatic species such as *p*-coumarate and ferulate, resulting in a 6-fold enrichment in LMW organic compounds relative to the crude APL. Experimental batch data were used to develop a detailed process model of an industrial scale, continuous membrane filtration system. The open-source model has several independent process inputs, such as the concentration of target compounds, feed flow rate, volume recovery, and membrane selectivity. This process model was used to show that the system has a low estimated energy demand (0.75 kW h m^{-3} permeate) and was used to identify primary cost drivers, including the membrane material cost. These results offer a key step towards a scalable, low energy, and cost-effective lignin MW fractionation method with implications for both improving product isolation from lignin and improving carbon yields across the biorefinery.

Received 7th January 2022,
Accepted 25th March 2022

DOI: 10.1039/d2gc00075j

rsc.li/greenchem

Introduction

Lignin is an abundant aromatic biopolymer that constitutes 15–30% of terrestrial plant biomass,[1] and the production of renewable chemicals from lignin is of interest to the biomass conversion community to improve both the economics and sustainability of biorefining.[2–11] Generally, the first step towards producing lignin-derived chemicals is a chemical reaction to depolymerize lignin into low molecular weight (LMW) (which we define here as <1000 Da) fragments. However, the resulting reaction product is often a heterogeneous mixture consisting of a HMW (>1000 Da) fraction that contains partially re- and depolymerized oligomeric and/or unreacted lignin, and a LMW fraction.[2,11]

For alkaline pretreated lignin (APL), which is distinct from kraft lignin in that it is sulfur-free, that is generated from grasses and agricultural residues, the stream is enriched in the salts of hydroxycinnamic acids. These hydroxycinnaminic acids include *p*-coumarate and ferulate, which originate as pendent groups bound to lignin and hemicellulose through ester linkages.[12] Additional compounds in APL derived from grasses and agricultural residues include acetate and hydroxy acid salts, such as lactate and glycolate, which are derived from hemicellulose deacetylation[13] and xylose degradation reactions, respectively.[14,15] These LMW compounds in APL can serve as renewable carbon sources for upgrading to a single product such as polyhydroxyalkanoates (PHAs) or aromatic catabolic products, such as muconic acid.[16–21] However, for many upgrading approaches, the HMW fraction

[a]*Renewable Resources and Enabling Sciences Center, National Renewable Energy Laboratory, Golden, CO, USA. E-mail: eric.karp@nrel.gov*
[b]*Advanced Biofuels and Bioproducts Process Development Unit, Biological Systems and Engineering Division, Lawrence Berkeley National Laboratory, Emeryville, CA, USA*

†Electronic supplementary information (ESI) available. See DOI: https://doi.org/10.1039/d2gc00075j

‡Current address: LanzaTech, 8045 Lamon Ave., Suite 400, Skokie, IL 60077.
§Current address: Chemical Engineering Dept., Colorado School of Mines, 1500 Illinois St., Golden, CO 80401.
¶Current address: Beyond Meat, 1325 E. El Segundo Blvd, El Segundo, CA 90245.

is underutilized as a carbon source.[2] This HMW fraction is problematic because it often repolymerizes during upgrading with the LMW compounds and thereby if separated from the LMW compounds upfront, it could be recycled to an appropriate depolymerization reaction to generate a larger slate of LMW compounds or it could be used directly in material applications.[22,23]

Accordingly, a key challenge in the valorization of lignin-rich streams, like APL, is the fractionation of the lignin-rich stream resulting from a lignin depolymerization reaction into a HMW lignin fraction from the LMW lignin fraction. Several separation approaches have been proposed to isolate lignin HMW and LMW fractions including distillation, extraction, precipitation, chromatography, and membrane separations.[24] Considering the high boiling point (>300 °C) and the low concentration (<1 wt%) of aromatic compounds, such as *p*-coumarate, in APL,[14] thermal approaches such as distillation are likely not viable because of excessive energy demand for solvent evaporation (water in the case of APL) and the likelihood for the thermal degradation of products. Successful isolation (>95% purity) of *p*-coumarate from corn stover was recently demonstrated by a combination of solvent extraction and crystallization.[25] However, to avoid excessive chemical demand, the process solvent needs to be recycled, for example by distillation, which leads to a high overall operating cost (~$3 per kg of hydroxycinnamic acid).[26–29] Another commonly employed approach for fractionation of alkaline liquors is precipitation *via* an acid gradient. The advantage of precipitation is the ease of operation at the bench scale, although there are several disadvantages limiting feasibility such as a resulting low-yield of LMW lignin-related compounds, excessive chemical consumption, and colloid formation.[24,26] Lastly, the fractionation of lignin from alkaline liquors has been demonstrated by size exclusion chromatography; however, the process requires expensive high pressure equipment for continuous processing *via* simulated moving bed (SMB), and clarification of the APL is needed prior to processing to prevent stationary phase fouling.[26,30,31] Considering the above challenges, APL fractionation *via* membrane separations is a promising approach because membrane systems operate non-thermally, have a low energy demand, and are widely used industrially, thus offering a short developmental timeline *via* commercially available membranes and modules.[23,24,32]

Membranes in the microfiltration (MF), ultrafiltration (UF), and nanofiltration (NF) range have been employed to recover defined molecular weight fractions from several lignin-rich streams.[10] Since the 1970s, MF has been proposed to recover HMW lignin from kraft and lignosulphonate pulping waste streams for material applications.[33] Recently, ceramic and polymeric membranes in the nanofiltration range have been employed to isolate LMW fractions from lignin rich liquors.[23,34,35] In one example, a NF membrane was applied to alkali-depolymerized kraft lignin to isolate a LMW fraction, which was then used as the feed for biological conversion.[36] The same work also suggests that the NF permeate has increased solubility compared to the feed liquor and thereby can be delivered to the bioreactor at a higher concentration than the original kraft lignin without precipitating. In another example, a nanofiltration process was demonstrated using polymeric membranes to isolate HMW and LMW lignin and the reaction solvent (propanol) from a reductive catalytic fractionation (RCF) process.[23] The report also included a techno-economic analysis (TEA) that estimated that an optimized process could operate with a total cost of $0.38 per kg of lignin-derived compound which is ~34% of the estimated product value ($1.11 per kg).[23] In light of this previous work, there is a continued need to better understand the potential for membrane fractionation in terms of the physical and chemical properties of the HMW and LMW fractions and to develop adaptable process models for agile TEA on various lignin-rich streams.[23,32,37]

To that end, we demonstrate a membrane process to separate APL into a HMW and LMW fraction (Fig. 1). We use data derived from MF and NF experiments process to build a two-stage process model and conduct a TEA to elucidate cost and performance drivers for APL fractionation. MF is employed in the first stage to remove bulk suspended solids from APL. The MF permeate was then subjected to a second NF stage, and we characterize the permeance and selectivity of ceramic NF membranes. The chemical composition, molecular weight distribution, and carbon content of the APL, retentate, and permeate were also evaluated to close mass balances on the process streams. Using the experimental compositional data, solvent, and solute permeance, a process model was built in Python to describe the two-stage MF/NF process. A preliminary TEA and energy analysis was completed based on the process model to define economic and energy drivers. The resulting filtration model presented in this work is a useful tool that is adaptable for other membranes with depolymerization feed

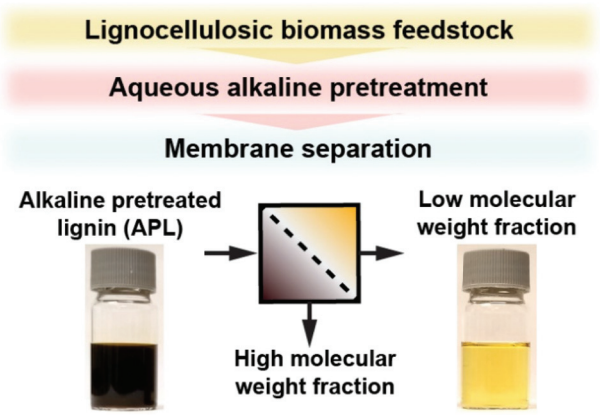

Fig. 1 Lignocellulosic biomass is first depolymerized using alkaline conditions into a heterogenous, lignin-rich alkaline pretreated liquor (APL). Membrane separation of the APL results in two fractions (1) a HMW retentate fraction composed primarily of partially depolymerized lignin and (2) a LMW permeate fraction containing aromatic compounds such as *p*-coumarate and ferulate (shown) that serve as a carbon source for biological and chemocatalytic funneling or downstream recovery and purification, towards renewable fuels and polymers.

streams beyond APL to examine LMW lignin recovery and associated TEA.

Results

Microfiltration and molecular weight separation of APL

APL was prepared from milled corn stover *via* alkaline depolymerization similar to our previous work and treated using centrifugation and MF to clarify the slurry prior to the NF screening experiments. The APL post pretreatment contained bulk unreacted corn stover solids removed by centrifugation. The aqueous fraction of APL, collected as the supernatant from centrifugation, contains a broad, non-normal distribution of molecular weights related with aromatic compounds as indicated by the high molecular weight average (M_w) ($M_w \sim 2002$) and polydispersity index (PDI) (PDI ~3.86) (Fig. 2 and Table 1) as determined by Gel Permeation Chromatography (GPC, absorbance at 260 nm). We then applied MF to remove fine suspended solids from the APL stream to prevent membrane fouling during downstream NF. For the MF, the retentate from a tangential flow system was recycled to the feed tank, and the permeate was collected in a separate vessel until the initial charge volume was reduced by at least 75 vol%. Subsequently, the permeate was collected and a small sample (<20 mL) was dried for GPC analysis. As shown in Fig. 2 and Table 1, MF reduces the M_w of lignin fraction of APL by 42% compared to the post-centrifugation APL.

The permeance of the flat sheet polymeric MF membrane was on average 17.4 L m^{-2} h^{-1} bar^{-1} (LMH per bar) taken over 6 hours of operation (Fig. S1†) (feed: 20 L).

We selected four tubular ceramic NF membranes for screening experiments with the aim to separate APL into a HMW and a LMW fraction. Ceramic membranes were chosen because they are known to be foulant resistant due to their hydrophilic nature and also because they have a long operational lifetime (>10 years) due to their chemical resistance, which will be needed for APL streams that generally have a pH > 10.[37,38]

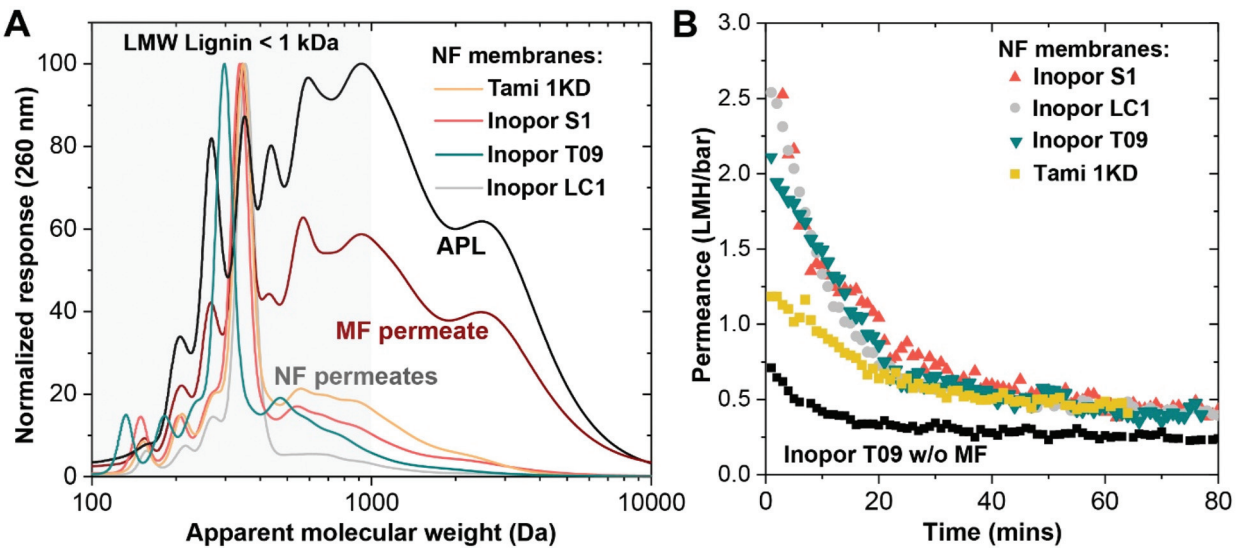

Fig. 2 (A) Gel-permeation chromatograms of the centrifuged APL supernatant, APL microfiltration (MF) permeate and APL nanofiltration (NF) permeates with different NF membranes. Here, MF pretreatment reduces the PDI and molecular weight of APL from 3.86 to 3.0 and 2002 to 1155 respectively. NF further reduced the PDI and molecular weight and removed >90% of HMW lignin oligomers. (B) Four nanofiltration (NF) ceramic membranes were screened for APL filtration with the Inopor membranes outperforming the Tami membrane by ~1.3× on average based on permeance (see Table 1). Each NF membrane has a high rejection of HMW lignin (>93%). MF pretreatment of APL increases the average NF permeance by 2.3-fold compared to NF of APL without pretreatment.

Table 1 APL and MF/NF permeate properties

Sample treatment	Membrane ID	Membrane material	Nominal cut-off	HMW rejection (%)	M_w	PDI	LMH per bar (average)
Centrifugation	n/a		n/a	n/a	2002	3.86	n/a
MF	MF	Alfa Laval MFP5	0.5 μm	2.7	1155	3.0	17.4
MF/NF	Tami 1KD	TiO_2	1 kDa	94.0	610	1.7	0.66
MF/NF	Inopor S1	SiO_2	600 Da	93.4	630	1.6	0.96
MF/NF	Inopor T09	TiO_2	450 Da	97.6	440	1.5	0.85
MF/NF	Inopor LC1	TiO_2	200 Da	98.6	380	1.4	0.84
NF (w/o MF)	Inopor T09	TiO_2	450 Da	92.5	460	1.4	0.37
NF (w/o MF), 70 °C	Inopor T09	TiO_2	450 Da	98.9	400	1.3	0.46

These properties are particularly attractive for processing lignin-rich streams, which have a propensity to foul membrane surfaces because of the oligomers present in the stream. Therefore, processing may require harsh physical and chemical membrane cleaning strategies to maintain membrane performance.[37] We also selected membranes with a nominal molecular weight cut-off (MWCO) in the range of approximately 200 Da to 1000 Da (Table 1). MWCO is defined as the molecular weight cut-off in which the membrane rejects 90% of a solute(s).[39]

To quantify and compare each membranes performance, we measured the membrane permeance and rejection of HMW APL. Rejection of HMW lignin was determined from normalized GPC curves with HMW lignin defined as integral of the signal associated with molecular weight >1000 Da on the chromatogram. The NF experiments were completed similarly to the MF experiments by using a bench-scale (200–500 mL) batch tangential flow system where the retentate was recycled back to the feed tank during operation. The NF permeate was collected continuously from the system until the initial charge was reduced by at least 75 vol%, at which time samples were collected for GPC analysis. The GPC traces of the NF permeate samples are shown in Fig. 2A. Table 1 lists the M_w and PDI of lignin-derived compounds in the NF permeates. As expected, the highest rejection and lowest M_w and PDI are achieved using the Inopor LC1 membrane which has the lowest nominal MWCO of 200 Da. All tested NF membranes have a HMW rejection between 92.5–98.6% (Table 1). Data of permeance over time for each NF membrane are shown in Fig. 2B and the average permeance over 1 hour of operation time of each membrane is reported in Table 1. In Fig. 2B, we show that the permeance of all NF membranes decreases to <0.5 LMH per bar over an hour of operation presumably due to membrane fouling as discussed below.

To examine the impact of the MF step on the performance and surface fouling during the NF process, the permeance of an NF membrane was determined with and without MF applied prior to NF. As seen in Fig. 2B, the NF permeance of APL without the application of MF is much lower (black squares) than when MF is applied. This difference is apparent within the averages (Table 1). The average NF permeance of the Inopor T09 membrane is 2.3-fold higher when MF is applied and the HMW rejection increases from 92.5% to 97.6%. To investigate the mechanism of fouling and the 2.3-fold increased permeance due to MF pretreatment (Table 1), we modelled the permeance decline behavior using the classical cake formation model and the intermediate pore blocking model (Fig. S2†).[40,41] Both models are time dependent and assume a filtration resistance due to membrane foulants with the cake formation model associated with faster permeance decline due to complete pore blocking. When APL is filtered without MF pretreatment, the permeance closely aligns with the cake formation model. However, when MF pretreatment was applied, the NF permeance decline closely fits the intermediate pore blocking model (Table S1†).[42] The transition from cake formation to the intermediate pore blocking phenomena is important because cake formation leads to ~2-fold faster permeance decline to 50% of the initial permeance (Fig. S2†) and a 2.3-fold lower average permeance.

Lastly, we examined the impact of temperature on the performance of the NF process. We found that by increasing the membrane module temperature to 70 °C, the permeance of the NF membrane increased from 0.37 LMH per bar to 0.46 LMH per bar and HMW rejection increased from 92.5 to 98.9% (Table 1). While increased membrane permeance and HMW rejection was gained by increasing temperature from 20 to 70 °C, we used samples collected from 20 °C filtrations to ensure sample integrity and to quantify LMW compounds as detailed in the next section.

Quantification of the LMW fraction of APL

The identification and quantification of small molecules in lignin depolymerization streams, such as APL, is challenging due to the chemical heterogeneity and the relative abundance of unaccounted HMW lignin which is ~90 wt% based on dry mass for APL.[14] Here, we quantify 22 compounds in APL *via* Liquid chromatography/refractive index detection (LC/RID) and ultra-high performance liquid chromatography with tandem mass spectrometry (UHPLC-MS/MS) *via* multiple reaction monitoring (MRM) and show a reduction in unaccounted HMW lignin when NF is applied *via* carbon tracking. The wt% of identified compounds was determined relative to the total carbon content of the sample by measuring the total carbon content of freeze-dried samples.

As expected based on previous works, compounds with the highest concentration in our APL include acetate, *p*-coumarate, lactate, glycolate, and ferulate (Table 2) (which are in there salt form in APL due to the presence of sodium hydroxide in APL (pH > 10)).[14,17] Acetate is the most abundant non-aromatic species in APL (acetate represents 47 wt% of the accounted mass) and is present in APL because of hemicellulose deacetylation during alkaline pretreatment processing. Additional carbohydrate-derived compounds include lactate and glycolate which originate in APL from sugar degradation products (*e.g.* xylan peeling reactions[43]). The most abundant aromatic products are *p*-coumarate (16 wt% of the accounted mass) and ferulate, which originate in APL from pendent groups whose ester linkages are cleaved from the lignin backbone during

Table 2 Primary compounds in APL and associated membrane permeate streams

	APL	MF APL	Tami 1KD	Inopor S1	Inopor T09	Inopor LC1
Major non-aromatic species (g L^{-1})						
Acetate	3.59	3.59	3.39	3.43	3.59	3.59
Lactate	0.52	0.52	0.45	0.47	0.45	0.52
Glycolate	0.22	0.22	0.17	0.19	0.19	0.22
Major aromatics species (g L^{-1})						
p-Coumarate	0.73	0.73	0.48	0.56	0.64	0.67
Ferulate	0.09	0.09	0.07	0.08	0.08	0.08
Total carbon (g L^{-1})	24.9	12.5	5.1	5.6	5.5	4.4

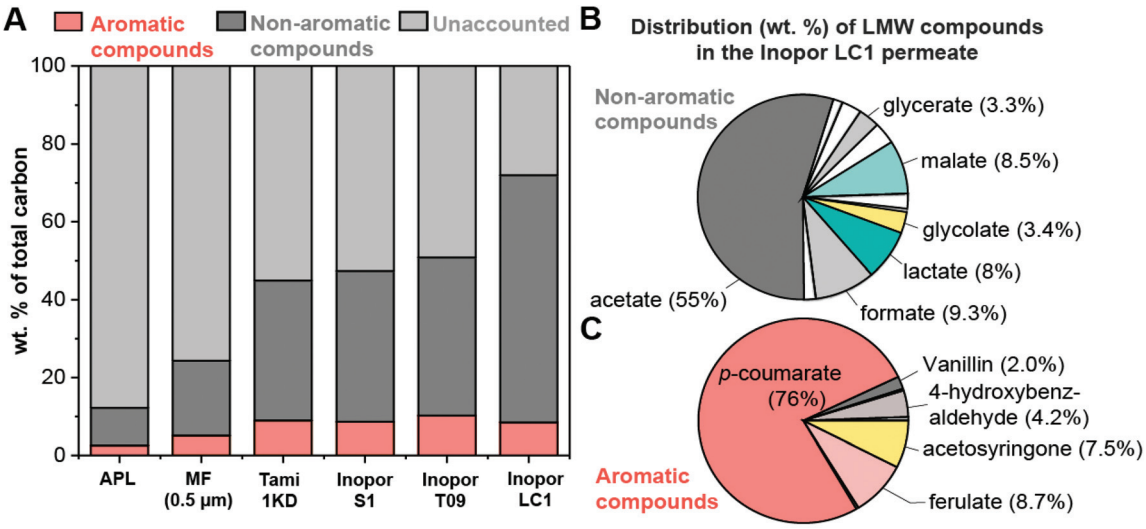

Fig. 3 (A) The wt% of LMW aromatic compounds, LMW non-aromatic compounds, and unaccounted carbon in APL and permeate samples relative to the total carbon in the sample. Tami and Inopor nanofiltration (NF) membranes reduce the unaccounted carbon from 88% in APL to <60% in permeate samples. (B) The charts show either the distribution of non-aromatic species (top) or (C) aromatic (bottom) species in the Inopor LC1 NF permeate sample.

alkaline pretreatment. In APL, the carbon associated with known and quantified compounds is only a small fraction of the total carbon in the sample; APL contains 24.9 g L^{-1} of carbon with 88 wt% of the carbon associated with unaccounted species (*i.e.* lignin oligomers, glucan, xylan, galactan (compositional analysis provided in Table S2†)). The remaining 12 wt% carbon is associated with: (1) non-aromatic carbohydrate-derived carboxylates, such as acetate, lactate, and glycolate and (2) aromatic compounds, such as *p*-coumarate and ferulate, as shown in Fig. 3A. The concentration of each compound quantified in the APL and permeates from each membrane is listed in Table S3.† To fractionate the LMW and HMW lignin in APL, MF followed by NF was applied on the APL sample as described above. We quantified the carbon content and lignin-related compounds in the MF and four NF permeates (Table 2 and Table S3†). The MF membrane reduced the total carbon content of APL by 50% (Table 2). Since the total carbon decreased by 50% due to MF treatment and the concentration of known compounds remains relatively constant upon MF treatment, the unaccounted lignin decreases from 88 wt% in APL to 76 wt% in the MF permeate (Fig. 3A) while the aromatic compounds comprise 5% of quantified carbon, and the non-aromatic species make up the remaining 19% of the quantified carbon.

The NF process, which uses the MF permeate as the feed, again reduces the carbon content by another ~50% and therefore the NF permeates have a carbon content that is only 18–23 wt% of the starting APL (Table 2) depending on the exact NF membrane used. The substantial reduction in total carbon in NF permeates compared to the MF sample results in a ~2-fold increase in the percentage of accounted carbon associated with LMW compounds relative to the total carbon (Fig. 3A). The Inopor LC1 has the least amount of unaccounted carbon, at 28 wt%, with 8.5% of carbon associated with aromatic compounds and the remaining 63.5% associated with non-aromatic species. Fig. 3B shows the distribution of tracked compounds relative to the weight of carbon associated with the category for the Inopor LC1 permeate. For the non-aromatic compounds (Fig. 3B), 55% of the quantified carbon is from acetate. For the aromatic family (Fig. 3C), 77% of the quantified carbon is associated with *p*-coumarate.

To qualitatively investigate the state of unaccounted HMW lignin in the NF permeates, we employed 2-dimensional Heteronuclear Single Quantum Coherence (HSQC) nuclear magnetic resonance (NMR) spectroscopy of the APL and the Inopor T09 NF permeate to examine the lignin chemistry. In the APL feed, there are signals at δ_C/δ_H 70–85/4.0–5.0 ppm associated with the presence of β-O-4 linkages. However, this signal is completely absent from the NF permeate sample (Fig. 4). Furthermore, for the APL feed, syringyl (S), guaiacyl (G), and *p*-hydroxyphenyl (H) moieties in the intact lignin polymer structure are clearly seen in the aromatic region (δ_C/δ_H 100–135/7.5–6.0 ppm) (Fig. S3†), while in the NF permeate, there is a disperse pattern in the aromatic region of the spectrum indicating a low concentration of intact lignin.

A continuous two-stage process for APL filtration

The results shown above capture the membrane performance of a laboratory-scale batch system; however, to estimate stream flowrates, compositions, and LMW compound recoveries for a two-stage continuous filtration process that can be used at industrial scale, a continuous process model was developed. Specifically, we modelled a two-stage process such that MF and NF modules are placed in series and linked *via* a process recycle loop that returns retentate from the NF stage to the feed of the MF stage (Fig. 5). The recycle loop essentially com-

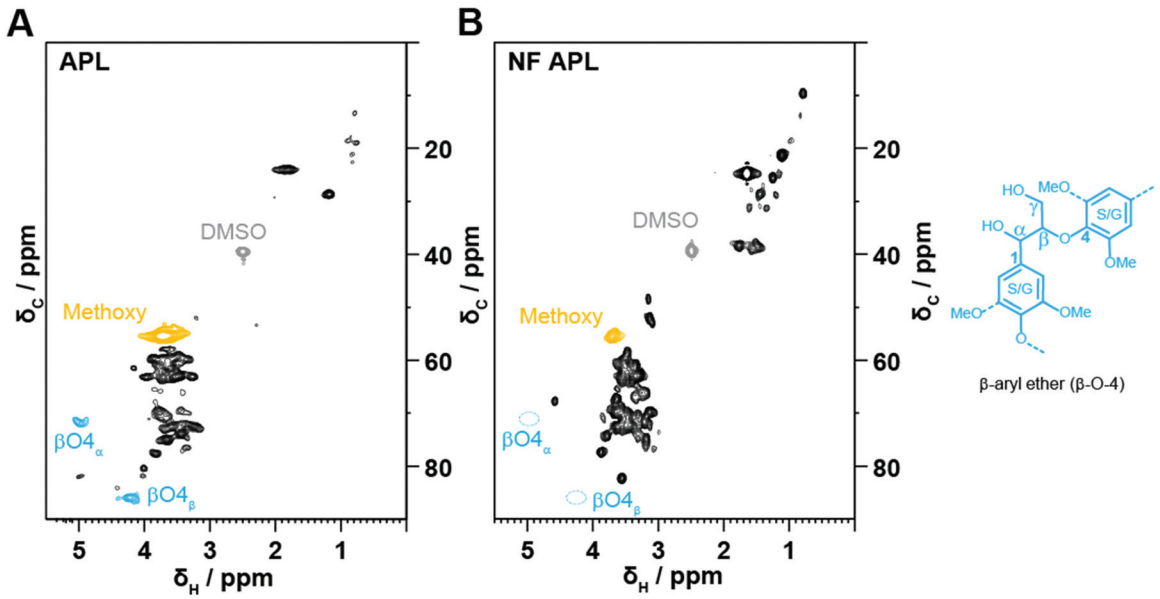

Fig. 4 2D HSQC NMR of the (A) APL starting material bond region; (B) NF permeate APL bond region. There is no evidence of remaining β-O-4 bonds in the NF permeate.

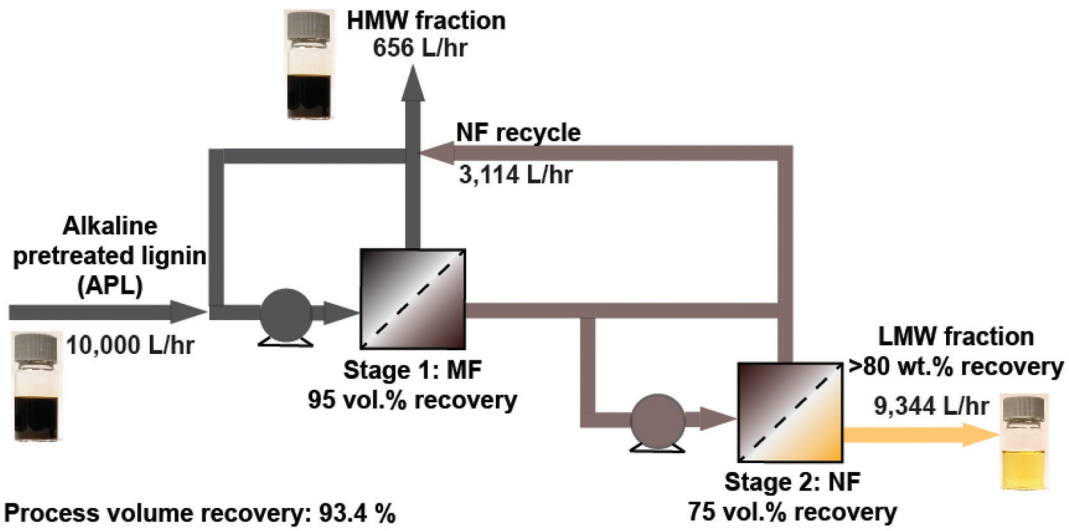

Fig. 5 A process flow diagram detailing the two-stage MF and NF process. The APL is pumped through the MF stage, where the HMW retentate is purged and the permeate is sent to the NF stage. The LMW NF permeate is collected while the retentate is recycled to the MF feed. Recirculation loops for both stages are included to achieve desired shear rates at the membrane wall during filtration. Stream flowrates (L h^{-1}) are included for MF and NF recoveries of 95 vol% and 75 vol%, respectively.

bines the retentate from both the MF and NF steps, thereby generating one HMW product stream. The model is based on results from the batch experimental data including membrane permeances and selectivity, and thereby is useful in comparing the performance of different membranes. A 'Process Model Operating Guide' is given in the ESI† detailing equations used, assumptions made, and how to access the Python codes. Briefly, we used the irreversible thermodynamic model adapted to a multicomponent NF process.[44,45] The process model assumes that the solvent and solute flux is proportional to the driving force, as detailed below and in the ESI.† The model was developed in Python and the code is publicly available on GitHub.

We first modelled the MF process selectivity and overall volume recovery based on the experimental findings. As shown in Table 2, MF removes suspended solids, and all tracked compounds have the same concentration in the feed and permeate and thus there is no rejection of these compounds during MF

and the LMW compound recovery is equal to the solvent recovery (95% in our process model). However, there is a rejection of unaccounted lignin as seen by the decreased carbon content of the permeate stream (Table 2) and the corresponding increase in the percent of carbon associated with tracked compounds (Fig. 3). From the concentration data, (Table S3†) the rejection coefficient of the MF membrane for unaccounted lignin was calculated (Table S4†) and used to calculate the MF retentate and permeate concentration of unaccounted lignin. The volumetric flowrate of the MF permeate stream relative to the feed stream flow is the volume recovery of the MF step and was set to 95 vol%. This value of 95 vol% for the MF stage was chosen since this recovery prevents the retentate from becoming excessively viscous (>100 cP) (Fig. S4 and S5†) which is preferred to avoid a high recirculation pump energy demand.

To determine the composition of the NF retentate and permeate, the selectivity must be determined for each compound. To simplify the NF process modelling, we chose to group compounds into two categories: (1) non-aromatic species and (2) aromatic species, as listed in Table S5.† We also determined the selectivity of the unaccounted lignin fraction for each membrane employed. The membrane selectivity of component *m* is defined as:

$$\alpha_m = \frac{K_{solv}}{K_m} \quad (1)$$

In eqn (1), α_m is the membrane selectivity of solute (Pa^{-1}), K_{solv} is the permeance of the solvent (kg Pa^{-1} m^{-2} s^{-1}), and K_m is the permeance of the solute (kg m^{-2} s^{-1}). Note the units of permeance depend on the driving force. The driving force for the solvent permeance is the difference between the transmembrane pressure drop and the osmotic pressure difference across the membrane, while the driving force for the LMW compounds and unaccounted lignin is the difference between the mass fraction of the compound at the membrane wall and in the permeate.[44] Smaller values ($\alpha_m \sim 1$) correspond to a solute permeance that is similar to the solvent (water, in this case) and conversely, larger values ($\alpha_m > 1$) correspond to a permeance that is less than water.

To calculate the selectivity of each tested membrane, we used our developed NF model with several initial conditions such as the feed concentration and initial permeance as well as the permeate experimental composition data (*e.g.* viscosity (Fig. S5†), density (Fig. S6†), and permeate concentrations (Fig. S7†)) as a function of volume recovery, the membrane selectivity of each solute can be estimated *via* eqn (S1)–(S14).† System level assumptions such as the module length and diffusivity are given in Tables S5 and S6.† The calculated membrane selectivity of the non-aromatic compounds, aromatic species, and unaccounted lignin for the four NF membranes screened are presented in Table 3. The Inopor LC1, which has a nominal MWCO of 200 Da, exhibits the highest HMW lignin rejection (98.6%) and has the highest selectivity value for unaccounted lignin. As expected, the Tami 1KD, which has the highest MWCO of 1000 Da of the screened membranes, has the lowest selectivity value for the unaccounted lignin.

Once the membrane selectivity for the NF stage is calculated from the batch experimental data, either a batch system with recycling or a two-stage continuous process model with recycling is used to calculate process outputs (membrane area, stream compositions, and LMW recovery as a function of volume recovery). We used the batch cross flow model to verify the model results by comparing to experimental data—the NF permeate concentrations of LMW compounds and unaccounted lignin predicted by the model were compared to the experimental batch measurements for the four membranes screened, and the comparison is shown in Fig. S7.† The two-stage model (process diagram in Fig. 5) was then implemented to estimate the stream flow rates (Table S7†), membrane area (Table S8†), compositions (Table 4, Fig. S7†), and LMW com-

Table 3 Membrane selectivity (α_m) (unit: Mass frac/Pa ($\times 10^{-7}$))

Component	Tami 1KD	Inopor S1	Inopor T09	Inopor LC1
Non-aromatic compounds	5.11	1.246	1.014	1.63
Aromatic compounds	11.5	33.69	10.29	36.2
Unaccounted	74.6	172.3	164.2	224.0

Table 4 Stream concentrations and LMW compound recovery estimated from the process model

NF membrane	Component	APL (g L^{-1})	NF permeate (g L^{-1})	NF recycle (g L^{-1})	Recovery (wt%)	Total LMW compound recovery (wt%)
Tami 1KD	Non-aromatics	6.1	5.1	6.5	78.3	77%
	Aromatics	0.9	0.6	1.1	66.7	
	Unaccounted	47.7	7.2	41.8	14.2	
Inopor S1	Non-aromatics	6.1	5.4	18.5	83.1	83%
	Aromatics	0.9	0.8	3.4	80.7	
	Unaccounted	47.7	9.2	90.4	17.9	
Inopor T09	Non-aromatics	6.1	5.3	18.2	81.6	82%
	Aromatics	0.9	0.8	2.8	83.0	
	Unaccounted	47.7	7.9	96.4	15.4	
Inopor LC1	Non-aromatics	6.1	5.6	19.2	86.4	84%
	Aromatics	0.9	0.6	4.2	65.0	
	Unaccounted	47.7	4.0	85.2	7.9	

pound recovery (Table 4) using a MF recovery of 95 vol% and a NF recovery of 75 vol%, which results in an overall process recovery of 93.4 vol% and is equivalent to the ratio between the NF permeate volume and the APL feed flow rates. Subsequently, this condition was chosen as a base case for TEA, which is detailed in the following section. The concentrations of the major process streams, the total LMW compound recovery, and HMW rejection estimated from the process model are summarized in Table 4.

TEA modeling and process energy demand

Economic drivers were identified by estimating the capital and operating expenses of an industrial scale, two-stage filtration process as developed above (Fig. 5) operating with a LMW compound recovery of 80%. The TEA boundary was limited to the membrane separation process and was considered independent of the upstream alkaline pretreatment process. First, we estimated the capital cost of a demonstration-scale plant (10 000 L h^{-1} feed of APL (*i.e.* a 200 ton per day of biomass plant capacity)).[6] Equipment capital expenses include the membrane modules, pumps, auxiliary equipment (*e.g.* feed and storage tanks) and were estimated for the two-stage process (Table S9†). The CAPEX of a 30-year plant is reported with units of \$ per m^3 of permeate using the volume of NF permeate generated by the plant as the basis. Additional financial assumptions such as the internal rate of return (IRR) and tax rate are listed in Table S10.†[6] For the TEA, we used four cases, differing by the selection of the NF membrane. The CAPEX for the two-stage process is 0.11–0.12 \$ per m^3 of permeate and is listed in Table 5 for each case.

The major operating expenses (OPEX) include the membrane replacement and energy demand expenses over the lifetime of the plant. The MF or NF operating cost is the cost of the MF or NF membrane materials needed throughout the lifetime of the plant accounting for the lifetime and raw material cost of the membranes. The membrane operating cost for the MF and NF process was estimated based on the amount of area needed. The MF operating expenses are 0.05 \$ per m^3 since the membrane area is the same for all cases. The NF operating expense ranges from 0.3 to 0.44 \$ per m^3 depending on the NF membrane (Table 5) with the best permeance membrane (Inopor S1) having the lowest operating cost because of the reduced required area compared to the other membrane processes. In addition, the combined energy consumption of the two-stage process was determined by estimating the pressure drop within the membrane modules and the required pumping duty (eqn (S18)–(S30)†). The total pumping duty was determined to be ~0.75 kW h m^{-3} which translates into an energy cost of ~0.05 \$ per m^3. The total expense (total CAPEX and OPEX) is shown in Table 5 and ranges from 0.51 to 0.67 \$ per m^3.

Additional lines in Table 5 are given to show the total expense normalized to the mass of total tracked LMW compounds (non-aromatic and aromatic) or to only aromatic compounds. The conversion from \$ per m^3 to \$ per kg is based on the concentration of compounds in the product stream (Table 4).

The proportion of a single expense (*i.e.* modules, energy, taxes, or the MF membranes) relative to the total expenses is shown in Fig. 6A for the process that uses the Inopor T09 NF membrane.

Because the NF operating costs are ~60% of the total expenses, a TEA sensitivity was performed to show the influence of parameters on the NF operating cost. Fig. 6B shows how the NF operating cost varies with respect to the NF membrane permeance and the total membrane material cost over the lifetime of the plant. The base case values used to generate Table 5 are shown as white points on the chart in Fig. 6B. A process specified with a permeance >0.5 LMH per bar and a membrane material cost <1000 \$ per m^2 is relatively well optimized (<\$0.55 per m^3) (for comparison industrial scale seawater reverse osmosis (RO) plants operate at (0.5–3.0 \$ per m^3).[46] In the discussion section, we further discuss the estimated total separation cost with respect to the economic value of the NF permeate stream and compare our results to other TEA cases that have been reported for lignin separations.

Membrane performance of a rotating ceramic disk (RCD) module

The TEA results in Fig. 6A indicate that the NF operating expense (61.5% of the total expense) is the major cost driver. Ultimately, NF operating cost is highly sensitive to the membrane cost per area which is set by the supplier and the cost of buying and replacing membranes. The total membrane area required is directly proportional to the permeance, and to reduce the total membrane area required, the membrane permeance must increase. However, a major challenge towards high permeance is membrane fouling that generally reduces the initial flux. An attractive option to mitigate fouling is the use hydro-dynamic membrane systems such as vibrating or

Table 5 Capital, operating, and total expense

	Tami 1KD	Inopor S1	Inopor T09	Inopor LC1
Total capital cost (\$ per m^3 permeate)	0.12	0.11	0.11	0.11
MF operating cost (\$ per m^3 permeate)	0.05	0.05	0.05	0.05
NF operating cost (\$ per m^3 permeate)	0.44	0.30	0.34	0.35
Electrical duty (\$ per m^3 permeate)	0.06	0.05	0.05	0.05
Total expenses (\$ per m^3 permeate)	0.67	0.51	0.55	0.56
Total expenses (\$ per kg LMW compounds)	0.12	0.08	0.09	0.09
Total expenses (\$ per kg aromatic compounds)	1.03	0.64	0.68	0.88

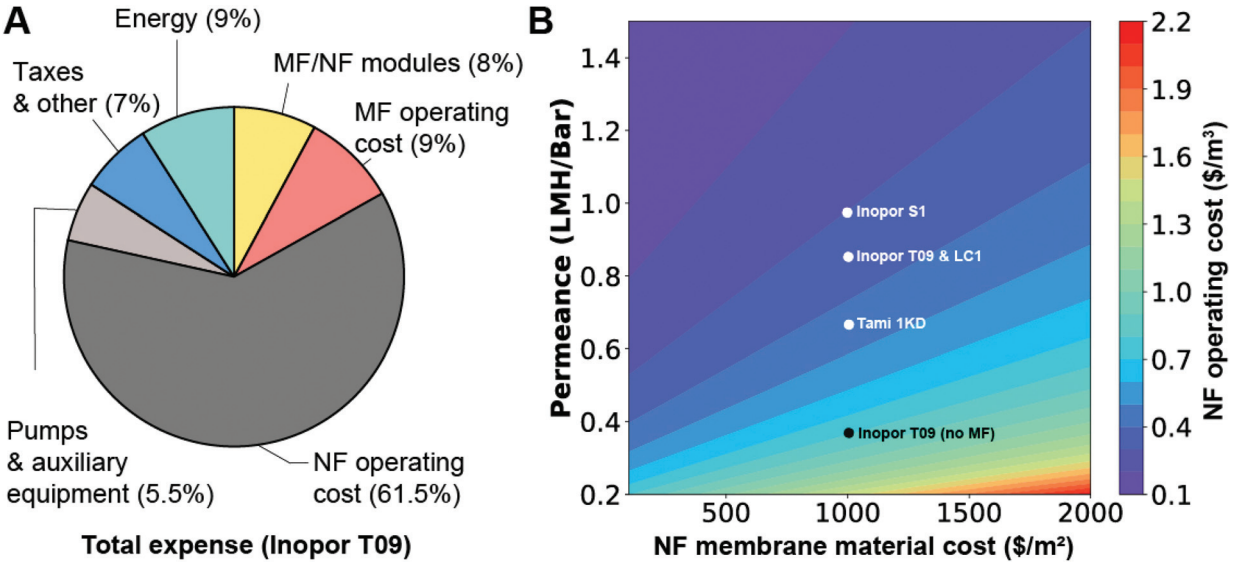

Fig. 6 (A) The portion of total expenses attributed to the NF/MF operating costs, the module costs, energy requirements or other expenses for a two-stage process utilizing a Inopor T09 NF membrane (B) sensitivity analysis showing the influence of NF permeance and membrane material cost on the NF operating cost.

rotating membranes. These systems achieve a high shear rate at the membrane surface which reduces foulants from attaching to the surface.[47] Another advantage of dynamic filtration over traditional cross flow is that process streams with high solids loading can be filtered. Below we present data from a rotating ceramic disk (RCD) module with the overall goal of decreasing operating costs by achieving high permeance while mitigating fouling.

To quantify and compare NF membrane performance of disk *vs.* tubular NF membranes, we measured the rejection of HMW lignin, permeance, and the M_w and PDI of the permeate from the RCD. In Fig. S8,† the NF disk membrane performance plotted with the performance of the Inopor S1 (600 Da MWCO). The NF disk membrane was fabricated by Fraunhofer IKTS and has a pore sizes of approximately 1 nm (~600 Da MWCO). The disk membrane achieved a HMW rejection of 93.0%, with the permeate having a M_w of 620 Da and a PDI of 1.9. These results are similar to the HMW rejection (93.4%), M_w (630 Da), and PDI (1.6) resulting from Inopor SI filtration. We show that the permeance of the disk membrane (5.0 LMH per bar on average) is substantial higher (~5-fold) than the permeance of the Inopor S1 tubular membrane (0.96 LMH per bar).

While the MF operating expense (9% of the total expense) is less of a cost driver compared with the NF operating expense, we validated the performance improvements that may be gained by using a disk MF membrane *vs.* a tubular MF. We used a ceramic disk MF membrane (see Materials and methods) to filter APL post-centrifugation. The permeance of the MF ceramic disk membrane was on average 41.9 LMH per bar over two hours. The measured MF permeance from the RCD is approximately 2-fold higher than the permeance of the flat sheet polymer MF membrane used over the same time frame.

In a TEA context, the permeance increases due to disk filtration has the potential to decrease the NF operating expense by approximately 5-fold, and the MF operating expense by 2-fold due to the lower membrane area requirements for these processes. However, further research is necessary to determine the associated capital expense of dynamic membrane modules and membranes and the overall impact on the total expense.

Discussion

The developed two-stage MF/NF membrane process, described above, is optimized to reject (up to 98.6%) HMW lignin from APL (Table 1). Our reported rejection (92.5–98.6%) of HMW lignin based on GPC analysis is similar to several membrane studies that have used ultra and NF membranes to filter HMW lignin. For example, a 87.4–94.6% rejection of HMW lignin has been achieved from a base-catalyzed depolymerization liquor *via* ultrafiltration.[48] Another study reported a 87.4–94.6% rejection of HMW oxidized kraft liquor *via* nanofiltration.[49] Lastly, a 98.5% rejection of HMW was previously reported from RCF oil using a three-stage polymeric NF membrane system.[23] Our results are in good agreement with previous reports showing that NF is an effective way to reject almost all of the HMW component present in lignin-rich streams, APL in our case. However, because membrane fractionation does not provide a perfect MWCO in one stage, our GPC traces show that there is aromatic lignin present in the NF permeate with MW between ~800–2000 Da (Fig. 2).

NF clearly enriches LMW species relative to the feed APL (Fig. 3). However, 28–55 wt% of the carbon in the permeate is 'unaccounted' lignin and is likely a mixture of lignin oligomers, glucan, xylan, galactan, *etc.* Our NMR spectroscopy results show that the APL feed has a strong signal associated with β-O-4 linkages, but that the NF permeate is apparently void of signal associated with β-O-4 linkages and thereby, the unaccounted lignin most likely does not contain β-O-4 linkages. However, additional studies are warranted to determine the composition and structure of the unaccounted lignin. Furthermore, to improve carbon yields within the biorefinery, the HMW retentate containing unaccounted lignin fraction could be sent to another lignin depolymerization reaction tuned to break β-O-4 bonds to increase LMW lignin and carbon yields. Another option for the HMW lignin retentate is various materials applications such as phenolic resins, emulsifiers, carbon fibers and polymer formulations.[50,51]

While membrane processes offer >80% recovery of LMW compounds, the selectivity and recovery of LMW compounds (aromatic *vs.* non-aromatics) were found to be substantially different (Tables 3 and 4). As previously reported by our group, several aromatic and hydroxy acid salts such as *p*-coumarate and acetate are present in APL.[14] Specifically, over 20 components including several mono-, hydroxy- and phenolic- acid salts were previously identified in APL *via* GC with time-of-flight mass spectrometry.[14] From our determined membrane selectivity results (Table 3), we can infer that the carbohydrate-derived carboxylates have a permeance close to the solvent and thus the selectivity values are close to 1. However, the aromatics are slower to permeate the membrane, which may be partially due to their higher molecular weight (164.1 Da for *p*-coumarate) relative to the solvent and non-aromatic species (60.1 Da for acetate), and thus the aromatics have a selectivity value that is ~10× higher than the non-aromatic species. The selectivity values for the non-aromatic and aromatic compounds are relatively constant across the four screened membranes (Table 3). Therefore, the best membrane option within the set examined here is driven by membrane flux rather than selectivity differences between the membranes as further explored in our TEA models.

Regarding the TEA, a major cost driver (~60% of the OPEX) of the process is the NF membrane cost (Fig. 6) over the plant lifetime (30 years) which includes the capital and replacement cost of the membrane. In the TEA, we based our estimate for the membrane raw material cost and lifetime on literature values. However, the current literature has a wide range of ceramic membrane costs from $200 to $1200 per m^2 and similarly wide range of membrane lifetimes from 6 to >25 years (current manufactures have a 20-year warranty) for ceramic membranes.[35,52,53] Because of the wide range reported for the cost and lifetime of membranes, we employed a sensitivity analysis to show how the total NF membrane expenses influence the total OPEX of the process. As shown in Fig. 6B, a process that has a permeance >0.5 LMH per bar and a total membrane material cost (over the lifetime of the plant) of <1000 $ per m^2 is relatively well optimized. Processes using NF polymeric membranes can use the same sensitivity map, using their respective permeance, lifetime (~1.5–2 years),[23,35] and material cost (20–300 $ per m^2 for spiral-wound modules).[54] Because of the shorter lifetime of a polymeric membrane, to match the NF material cost of the Inopor S1 membrane ($900 per m^2 over the lifetime of the plant), a polymeric membrane with a lifetime of 1.5 years must have at most a price point of $45 per m^2 which is well within the literature range (20–300 $ per m^2).[54]

To put our developed two-stage membrane system in context of other lignin fractionation approaches, the operating expenses are directly compared below, with results that are encouraging for simple membrane systems (less than three stages) compared to extractive methods. Membrane systems that require additional stages, such as the three-stage polymeric NF process for RCF oil developed previously, have more required membrane area, necessitating high permeance (5 LMH per bar) to reduce operating costs to $0.38 per kg monomers in the permeate.[23] In comparison to extractive processes, an ethanol precipitation process was designed to isolate neat *p*-coumarate and ferulate. That extractive approach includes a solvent recycling process and multiple acid/base input streams to recover the free acid form of the aromatic products, resulting in a low-pressure steam (LPS) cost alone of $3 per kg allocated for distillation processes to recycle the solvent. Another disadvantage of extractive approaches is that solvent losses must be kept to a minimum (<0.1%) to avoid excessive raw material costs.[28] The two-stage APL process has a relatively low operating cost (as low as $0.08 per kg LMW compounds) (Table 5). However, the operating cost reported in Table 5 ranges from $0.08 to $1.03, depending on the target products from APL and the overall feasibility depends greatly on the commercial value of the small molecule products.

Because the filtration process generates a mixed composition stream and not a pure product stream, the processing cost of the filtration must be considered against the market value of the final obtained product and the cost of the downstream process aimed to generate a marketable product. There are generally two downstream methods that are employed after filtration: (1) upgrading of the permeate *via* funneling toward a specific product such as adipic acid,[36,55] or (2) isolation of a specific aromatic species within the permeate *via* chromatography.[31] In the case of funneling, assuming all of LMW compounds in the permeate are converted to a single product, the 2-stage filtration cost (0.08 $ per kg LMW compounds) (Table 5) is small (4.5%) relative to the product selling price ($1.8 per kg for adipic acid).[55] In the case of chromatography, assuming all of the aromatics are recovered in isolated fractions, the 2-stage filtration cost (0.64 $ per kg of aromatic species) is approaching the final product value cost (reported to be as low as $1 per kg).[28] In addition, the TEA of the downstream processes such as biological conversion, chromatography, and/or water evaporation (~1 $ per m^3)[56] may greatly impact feasibility.[57]

Lastly, a key challenge with reducing operating costs is to maintain a high permeance by preventing fouling. Our process

and TEA models assume a constant MF and NF permeance during operation. However, the permeance of the membrane process is often reduced over time due to foulants in the APL. Primary foulants are likely to be the HMW fraction containing oligomers (Table S2†) and silica in the retentate streams. Agriculture residue such as corn stover are known to contain silica as part of the ash.[58] Silica and polysaccharides have previously been identified as foulants in the ultrafiltration of alkaline pulp from alkaline bleach generated from sulfite pulping.[59] While the permeance of the membrane could be maintained by increasing the transmembrane pressure (constant flux operation), fouling mitigation strategies such as backflushing and chemical cleaning are commonly used to prevent excessive membrane fouling. For example, a 48% increase in the average flux of wastewater from a sulfite pulp process was achieved *via* backflushing a ceramic membrane for 10 seconds every 120 minutes.[37] In terms of a target permeance for economically competitive processing, a target of 5 LMH per bar was previously noted by Sultan *et al.* (2019) which could reduce RCF membrane processing expenses to $0.38 per kg of dried phenolic compounds.[23] Using our RCD data (5.0 LMH per bar permeance for NF), the membrane processing expenses can potentially be reduce to $0.27 per kg of aromatics. However, additional unit operations are needed to remove water and unwanted salts (NaOH) from the APL product stream before upgrading reactions.

Conclusion

Membrane processes are emerging as a robust and low-cost fractionation method to generate enriched LMW and HMW lignin-derived fractions that are ideal for chemical production. Our work on membrane fractionation shows that a two-stage MF/NF filtration system rejects up to 98.6% HMW lignin from APL and has a recovery of up to 84% for LMW compounds. Because of the excellent rejection of HMW lignin, 72 wt% of the total carbon in the permeate is associated with tracked compounds, which represents a 6-fold enrichment over the original APL stream. Additionally, our TEA and energy analysis was developed *via* a process modelling approach (available on GitHub‖) and indicate a low process energy demand of ~0.75 kW h m^{-3} and a total expense ranging from 0.51 to 0.67 $ per m^3. While the NF operating cost was found to be a cost driver (>60% of the total expense), based on our sensitivity analysis, minimized NF operating cost (<$0.55 per m^3) occurs when the NF permeance is >0.5 LMH per bar and the membrane material cost <1000 $ per m^2. Furthermore, membrane selectivity and permeance data used within our process model and TEA indicate that membrane fractionation is economically feasible with a total expense that is less than 5% of the final product selling price if 100% of the fractionated LMW compounds in the NF permeate are converted to a single product, such as adipic acid. Together, the experimental results and process model are key steps towards improving the lignin-to-chemicals valorization chain and may increase carbon yield within the biorefinery without a substantial economic penalty.

‖ Python codes are available on GitHub.com (NREL-SEPCON – **https://github.com/NREL-SEPCON/Lignin-Filtration**).

Materials and methods

Alkaline pretreatment lignin (APL)

Corn stover provided by Idaho National Laboratory (INL) was milled to 3/16 inch and air-dried. The milled feedstocks were stored at 4 °C with room humidity maintained at 64–70% until pretreatment. The milled corn stover was pretreated in a 10 L Parr vessel (Parr Instrument Company, model 4555-58, Moline, IL, USA) for 30 min at 130 °C using a 10 wt% of solids and a NaOH loading of 85 mg g^{-1} dry biomass as previously reported.[15] After the reactor was cooled down to room temperature, the slurry was transferred out and centrifuged (Thermo Scientific, Sorvall RC 12BP+) for 10 min at 4800 RPM to obtain the lignin-rich supernatant. The supernatant (pH 10.4) was then prefiltered with a 2.7 μm microfiber filter (GE, Grade GF/D) to remove any remaining large, suspended particles.

Microfiltration (MF) of APL

Alfa Laval M20 unit (LabStak M20-0.72, Alfa Laval, Lund, Sweden) was employed for the microfiltration test. 20 Liters of APL was filtered by 0.5 μm membranes (Alfa Laval, Lund, Sweden) at 20 °C. The surface area of the membranes was 0.072 m^2. The transmembrane pressure was 2.4 bar and the crossflow rate was set to 5.7 L min^{-1}. 17.1 L of permeate was collected and used as the feed material for nanofiltration tests. Prior to each experiment, the membranes were cleaned and prepared according to the manufacturer's instructions (washed with DI water, 0.1 mM NaOH, and then finally with DI until the permeate was pH 7).

Nanofiltration (NF) of APL

A 250 mm × 10 mm nanofiltration membrane module was purchased from Inopor GmbH (Scheßlitz, Germany). The membrane module was connected to a recirculation pump (Micropump, Vancouver, WA), a HPLC pump (Cole Parmer (Vernon Hills, IL), and a 500 mL feed vessel. Single channel (250 × 10 × 7 mm) ceramic membranes (Material and property information is given in Table 2 and Table S11†) were purchased from Inopor and Sterlitech (Kent, WA). After the system was cleaned, ~250 mL of stock APL solution post MF was added to the feed vessel. The recirculation loop was maintained at 200 psig (N_2 tank supply) with the recirculation loop flow rate set to 420 mL min^{-1} and the HPLC pump was set to 8–10 mL min^{-1}. Filtration was carried out at 20 °C. The permeate was collected on a scale with readouts every 1 minute. Permeate samples were collected in 25 mL increments until a 75% volume reduction of the initial change was achieved. Feed, final retentate, and final permeate sample at 75% volume reduction were analyzed by GPC, LC/MS, and for

carbon content as described below. Samples at 25, 50, and 70% volume reduction were also quantified by LC/MS to determine the membrane selectivity. Prior to each experiment, the membranes were cleaned (washed with DI water, then backflushed overnight with 0.25 M NaOH with 1% Liquinox, and then finally with DI until the permeate was pH 7). The water flux was measured before each experiment (Table S1†) to ensure that the membranes were clean.

Gel permeation chromatography (GPC)

30 mg of each of APL permeate, feed, and retentate sample was acetylated in a mixture of pyridine (0.5 mL) and acetic anhydride (0.5 mL) at 40 °C for 24 h with stirring. The reaction was terminated by addition of methanol (0.2 mL). The acetylation reagents were removed by evaporation under a stream of nitrogen gas. The samples were further dried in a vacuum oven at 40 °C overnight. The dried, acetylated lignin samples were dissolved in tetrahydrofuran (2.5 ml). The dissolved samples were filtered through 0.45 μm nylon membrane syringe filters before GPC analysis. GPC analysis was performed using an Agilent HPLC with 3 GPC columns (Polymer Laboratories, 300 × 7.5 mm) packed with polystyrene-divinyl benzene copolymer gel (10 μm beads) having nominal pore diameters of 10^4, 10^3 and 50 Å. The eluent was THF with 1.0 mL min^{-1} flow rate. An injection volume was 25 μL. The HPLC was attached to a diode array detector measuring absorbance at 260 nm (bandwidth 80 nm). Retention time was converted into molecular weight (MW) by applying a calibration curve established using polystyrene standards of known molecular weight (9.8×10^5 to 580 Da) plus toluene (92 Da).

Liquid chromatography/refractive index detection (LC/RID)

Aliphatic acid analysis was perform using an Agilent 1200 HPLC system (Agilent Technologies, Santa Clara, CA) paired with a refractive index detector (RID). All samples and analytical standards were injected at a volume of 20 μL onto an Aminex HPX-87H Ion Exclusion column 300 × 7.8 mm (Bio-Rad, Hercules, CA). The column temperature was maintained at 55 °C, and separation was achieved using a mobile phase of 0.02 N sulfuric acid held isocaratically at 0.5 mL min^{-1} for a total runtime of 30 minutes. Unique compound standards were obtained from Sigma Aldrich (St Louis, MO) and combined to create a calibration curve ranging from 0.125 g L^{-1} to 5 g L^{-1}. Seven total calibration levels were used to construct a curve with a linear r^2 coefficient greater than 0.995 for each analyte. Calibration verification standards (CVS) were injected at an interval of every 15 injections to verify instrument stability.

Analysis of lignin-related aromatic compounds by UHPLC-MS/MS (MRM)

Aromatic compounds derived from lignin were analyzed by ultra high-performance liquid chromatography (UHPLC) tandem mass spectrometry as described in Salvachúa *et al.* (2020)[60] with the substitution of mobile phase A from 4 mM ammonium formate to 0.1% formic acid. Aromatic standards were used to optimize multiple reaction monitoring (MRM) transitions and collison energies for compounds of interest and deuterated 4-hydroxybenzoic-2,3,5,6-d_4 acid utilized as an internal standard for all compounds. Quantifying and qualifying MRM transitions for each analyte and the respective collision energy and fragmentor voltages are presented previously in ESI Table S1† in del Cerro *et al.* (2021).[61] A CVS was injected every 10 samples to monitor instrument drift and quantitation was achieved by unique internal standard calibration curves.

Carbon analysis

Feed, retentate, and permeate samples were freeze-dried for elemental analysis. Ultimate analysis was performed using a LECO Series 628 Carbon, Hydrogen, Nitrogen Determinator.

NMR spectroscopy

Samples received were solubilized in DMSO-d_6. HSQC NMR spectra were acquired at 25 °C on either a Bruker Avance 400 MHz or 600 MHz spectrometer using a room temperature broadband probe. Spectra were acquired with 1024 points and a SW of 12 ppm in the F2 (1^H) dimension and 256 points and SW of 220 ppm in the F1 (13^C) dimension using a standard phase sensitive, gradient selected pulse sequence. All spectral processing was done in Bruker Topspin 3.6.1 and peaks were identified based on previous work.

Viscosity

All viscosity measurements were taken using a Brookfield DV2T – LV Viscometer. A single point method with an end condition time of one minute was employed and spindles CP-40, V-72 and V-74 were used. All measurements were taken at room temperature using rotational speeds between 10 and 200 rpm.

Compositional analysis

Performed as described in Sluiter *et al.* (2008).[62]

Ceramic disk filtration of APL

A rotating ceramic disk module (152/S, Andritz, Austria) was employed for MF and NF. Centrifuged APL broth was filtered through a 0.2 μm ceramic disk membrane (0.034 m^2) (Andritz, Austria) operating at 1100 rpm and 20 °C. The transmembrane pressure was set to 1.1 bar and 3 L of feed was processed. The ceramic disk NF membrane used in this work was fabricated by Fraunhofer IKTS and has an approximate pore size of 1 nm (~600 Da MWCO). During NF, the 152/S module was operated at 5 Bar, 100 rpm, and 20 °C. Prior to filtration, the membranes were washed with 0.25 M NaOH for 12 hours. The membrane system was then washed with DI water until a pH < 8 was achieved.

Conflicts of interest

There are no conflicts of interest to declare.

Acknowledgements

The research reported in this paper was sponsored by the U.S. Department of Energy (DOE), Energy Efficiency and Renewable Energy Office, Bioenergy Technologies Office (BETO) under the BETO Bioprocessing Separations Consortium *via* Contract No. DE-AC36-08GO28308 with the National Renewable Energy Laboratory and NL0032351 with the Lawrence Berkeley National Laboratory. The authors gratefully acknowledge the support of Nichole Fitzgerald and Gayle Bentley at BETO. We thank Lauren Valentino at Argonne National Laboratory for her leadership in the Separations Consortium and Laura Hollingsworth for a critical review of the manuscript. The views expressed in the article do not necessarily represent the views of the U.S. Department of Energy or the U.S. Government. The authors from the ABPDU also acknowledge the funding from the American Recovery and Reinvestment Act.

Notes and references

1 S. P. Chundawat, G. T. Beckham, M. E. Himmel and B. E. Dale, Deconstruction of lignocellulosic biomass to fuels and chemicals, *Annu. Rev. Chem. Biomol. Eng.*, 2011, **2**, 121–145.

2 G. T. Beckham, C. W. Johnson, E. M. Karp, D. Salvachúa and D. R. Vardon, Opportunities and challenges in biological lignin valorization, *Curr. Opin. Biotechnol.*, 2016, **42**, 40–53.

3 A. J. Ragauskas, G. T. Beckham, M. J. Biddy, R. Chandra, F. Chen, M. F. Davis, B. H. Davison, R. A. Dixon, P. Gilna, M. Keller, P. Langan, A. K. Naskar, J. N. Saddler, T. J. Tschaplinski, G. A. Tuskan and C. E. Wyman, Lignin valorization: improving lignin processing in the biorefinery, *Science*, 2014, **344**(6185), 1246843.

4 R. Rinaldi, R. Jastrzebski, M. T. Clough, J. Ralph, M. Kennema, P. C. Bruijnincx and B. M. Weckhuysen, Paving the way for lignin valorisation: recent advances in bioengineering, biorefining and catalysis, *Angew. Chem., Int. Ed.*, 2016, **55**(29), 8164–8215.

5 Z. Sun, B. Fridrich, A. de Santi, S. Elangovan and K. Barta, Bright side of lignin depolymerization: toward new platform chemicals, *Chem. Rev.*, 2018, **118**(2), 614–678.

6 R. Davis, L. Tao, E. Tan, M. Biddy, G. Beckham, C. Scarlata, J. Jacobson, K. Cafferty, J. Ross and J. Lukas, *Process design and economics for the conversion of lignocellulosic biomass to hydrocarbons: dilute-acid and enzymatic deconstruction of biomass to sugars and biological conversion of sugars to hydrocarbons*, National Renewable Energy Lab.(NREL), Golden, CO (United States), 2013.

7 A. Corona, M. J. Biddy, D. R. Vardon, M. Birkved, M. Z. Hauschild and G. T. Beckham, Life cycle assessment of adipic acid production from lignin, *Green Chem.*, 2018, **20**(16), 3857–3866.

8 K. Huang, P. Fasahati and C. T. Maravelias, System-level analysis of lignin valorization in lignocellulosic biorefineries, *iScience*, 2020, **23**(1), 100751.

9 S. S. Wong, R. Shu, J. Zhang, H. Liu and N. Yan, Downstream processing of lignin derived feedstock into end products, *Chem. Soc. Rev.*, 2020, **49**(15), 5510–5560.

10 Z. Sun, J. Cheng, D. Wang, T. Q. Yuan, G. Song and K. Barta, Downstream Processing Strategies for Lignin–First Biorefinery, *ChemSusChem*, 2020, **13**(19), 5134–5134.

11 W. Schutyser, a. T. Renders, S. Van den Bosch, S.-F. Koelewijn, G. Beckham and B. F. Sels, Chemicals from lignin: an interplay of lignocellulose fractionation, depolymerisation, and upgrading, *Chem. Soc. Rev.*, 2018, **47**(3), 852–908.

12 J. Ralph, Hydroxycinnamates in lignification, *Phytochem. Rev.*, 2010, **9**(1), 65–83.

13 H. V. Scheller and P. Ulvskov, Hemicelluloses, *Annu. Rev. Plant Biol.*, 2010, **61**(1), 263–289.

14 E. M. Karp, C. T. Nimlos, S. Deutch, D. Salvachúa, R. M. Cywar and G. T. Beckham, Quantification of acidic compounds in complex biomass-derived streams, *Green Chem.*, 2016, **18**(17), 4750–4760.

15 E. M. Karp, B. S. Donohoe, M. H. O'Brien, P. N. Ciesielski, A. Mittal, M. J. Biddy and G. T. Beckham, Alkaline pretreatment of corn stover: bench-scale fractionation and stream characterization, *ACS Sustainable Chem. Eng.*, 2014, **2**(6), 1481–1491.

16 J. G. Linger, D. R. Vardon, M. T. Guarnieri, E. M. Karp, G. B. Hunsinger, M. A. Franden, C. W. Johnson, G. Chupka, T. J. Strathmann and P. T. Pienkos, Lignin valorization through integrated biological funneling and chemical catalysis, *Proc. Natl. Acad. Sci. U. S. A.*, 2014, **111**(33), 12013–12018.

17 D. Salvachúa, E. M. Karp, C. T. Nimlos, D. R. Vardon and G. T. Beckham, Towards lignin consolidated bioprocessing: simultaneous lignin depolymerization and product generation by bacteria, *Green Chem.*, 2015, **17**(11), 4951–4967.

18 D. R. Vardon, M. A. Franden, C. W. Johnson, E. M. Karp, M. T. Guarnieri, J. G. Linger, M. J. Salm, T. J. Strathmann and G. T. Beckham, Adipic acid production from lignin, *Energy Environ. Sci.*, 2015, **8**(2), 617–628.

19 D. Salvachúa, T. Rydzak, R. Auwae, A. De Capite, B. A. Black, J. T. Bouvier, N. S. Cleveland, J. R. Elmore, A. Furches and J. D. Huenemann, Metabolic engineering of Pseudomonas putida for increased polyhydroxyalkanoate production from lignin, *Microb. Biotechnol.*, 2020, **13**(1), 290–298.

20 J. R. Elmore, G. N. Dexter, D. Salvachúa, M. O'Brien, D. M. Klingeman, K. Gorday, J. K. Michener, D. J. Peterson, G. T. Beckham and A. M. Guss, Engineered Pseudomonas putida simultaneously catabolizes five major components of corn stover lignocellulose: Glucose, xylose, arabinose, p-coumaric acid, and acetic acid, *Metab. Eng.*, 2020, **62**, 62–71.

21 D. Salvachúa, C. W. Johnson, C. A. Singer, H. Rohrer, D. J. Peterson, B. A. Black, A. Knapp and G. T. Beckham,

Bioprocess development for muconic acid production from aromatic compounds and lignin, *Green Chem.*, 2018, **20**(21), 5007–5019.

22 J. H. Lora and W. G. Glasser, Recent industrial applications of lignin: a sustainable alternative to nonrenewable materials, *J. Polym. Environ.*, 2002, **10**, 39–48.

23 Z. Sultan, I. Graça, Y. Li, S. Lima, L. G. Peeva, D. Kim, M. A. Ebrahim, R. Rinaldi and A. G. Livingston, Membrane Fractionation of Liquors from Lignin–First Biorefining, *ChemSusChem*, 2019, **12**(6), 1203–1212.

24 T. Pang, G. Wang, H. Sun, W. Sui and C. Si, Lignin fractionation: Effective strategy to reduce molecule weight dependent heterogeneity for upgraded lignin valorization, *Ind. Crops Prod.*, 2021, **165**, 113442.

25 V. I. Timokhin, M. Regner, A. H. Motagamwala, C. Sener, S. D. Karlen, J. A. Dumesic and J. Ralph, Production of p-coumaric acid from corn GVL-lignin, *ACS Sustainable Chem. Eng.*, 2020, **8**(47), 17427–17438.

26 J. S. Rodrigues, V. Lima, L. s. C. Araújo and V. R. Botaro, Lignin Fractionation Methods: Can Lignin Fractions Be Separated in a True Industrial Process?, *Ind. Eng. Chem. Res.*, 2021, 10863–10881.

27 X. Meng, A. Parikh, B. Seemala, R. Kumar, Y. Pu, C. E. Wyman, C. M. Cai and A. J. Ragauskas, Characterization of fractional cuts of co-solvent enhanced lignocellulosic fractionation lignin isolated by sequential precipitation, *Bioresour. Technol.*, 2019, **272**, 202–208.

28 S. D. Karlen, P. Fasahati, M. Mazaheri, J. Serate, R. A. Smith, S. Sirobhushanam, M. Chen, V. I. Tymokhin, C. L. Cass and S. Liu, Assessing the viability of recovery of hydroxycinnamic acids from lignocellulosic biorefinery alkaline pretreatment waste streams, *ChemSusChem*, 2020, 2012–2024.

29 M. Yang, M. S. U. Rehman, T. Yan, A. U. Khan, P. Oleskowicz-Popiel, X. Xu, P. Cui and J. Xu, Treatment of different parts of corn stover for high yield and lower polydispersity lignin extraction with high-boiling alkaline solvent, *Bioresour. Technol.*, 2018, **249**, 737–743.

30 E. Gomes and A. Rodrigues, Lignin biorefinery: Separation of vanillin, vanillic acid and acetovanillone by adsorption, *Sep. Purif. Technol.*, 2019, **216**, 92–101.

31 I. F. Mota, P. R. Pinto, J. M. Loureiro and A. E. Rodrigues, Purification of syringaldehyde and vanillin from an oxidized industrial kraft liquor by chromatographic processes, *Sep. Purif. Technol.*, 2020, **234**, 116083.

32 D. Humpert, M. Ebrahimi and P. Czermak, Membrane technology for the recovery of lignin: A review, *Membranes*, 2016, **6**(3), 42.

33 A.-S. Jönsson and O. Wallberg, Cost estimates of kraft lignin recovery by ultrafiltration, *Desalination*, 2009, **237**(1–3), 254–267.

34 K. Servaes, A. Varhimo, M. Dubreuil, M. Bulut, P. Vandezande, M. Siika-Aho, J. Sirviö, K. Kruus, W. Porto-Carrero and B. Bongers, Purification and concentration of lignin from the spent liquor of the alkaline oxidation of woody biomass through membrane separation technology, *Ind. Crops Prod.*, 2017, **106**, 86–96.

35 A. Arkell, J. Olsson and O. Wallberg, Process performance in lignin separation from softwood black liquor by membrane filtration, *Chem. Eng. Res. Des.*, 2014, **92**(9), 1792–1800.

36 O. Y. Abdelaziz, K. Ravi, M. Nöbel, P. Tunå, C. Turner and C. P. Hulteberg, Membrane filtration of alkali-depolymerised kraft lignin for biological conversion, *Bioresour. Technol.*, 2019, **7**, 100250.

37 A. Bokhary, A. Tikka, M. Leitch and B. Liao, Membrane fouling prevention and control strategies in pulp and paper industry applications: A review, *J. Membr. Sci. Res.*, 2018, **4**(4), 181–197.

38 S. M. Samaei, S. Gato-Trinidad and A. Altaee, The application of pressure-driven ceramic membrane technology for the treatment of industrial wastewaters–A review, *Sep. Purif. Technol.*, 2018, **200**, 198–220.

39 C. J. Yehl and A. L. Zydney, Characterization of dextran transport and molecular weight cutoff (MWCO) of large pore size hollow fiber ultrafiltration membranes, *J. Membr. Sci.*, 2021, **622**, 119025.

40 S. Mondal and S. De, A fouling model for steady state crossflow membrane filtration considering sequential intermediate pore blocking and cake formation, *Sep. Purif. Technol.*, 2010, **75**(2), 222–228.

41 R. C. Daniel, J. M. Billing, R. L. Russell, R. W. Shimskey, H. D. Smith and R. A. Peterson, Integrated pore blockage-cake filtration model for crossflow filtration, *Chem. Eng. Res. Des.*, 2011, **89**(7), 1094–1103.

42 W. H. Press, H. William, S. A. Teukolsky, A. Saul, W. T. Vetterling and B. P. Flannery, *Numerical recipes 3rd edition: The art of scientific computing*, Cambridge university press, 2007.

43 M. Paananen, S. Rovio, T. Liitiä and H. Sixta, Stabilization, degradation, and dissolution behavior of Scots pine polysaccharides during polysulfide (K-PS) and polysulfide anthraquinone (K-PSAQ) pulping, *Holzforschung*, 2015, **69**(9), 1049–1058.

44 P. C. Wankat, *Separation process engineering*, Pearson Education, 2006.

45 K. Spiegler and O. Kedem, Thermodynamics of hyperfiltration (reverse osmosis): criteria for efficient membranes, *Desalination*, 1966, **1**(4), 311–326.

46 Y. Okamoto and J. H. Lienhard, How RO membrane permeability and other performance factors affect process cost and energy use: A review, *Desalination*, 2019, **470**, 114064.

47 S. Bhattacharjee, S. Datta and C. Bhattacharjee, Performance study during ultrafiltration of Kraft black liquor using rotating disk membrane module, *J. Cleaner Prod.*, 2006, **14**(5), 497–504.

48 K. Li, B. Al-Rudainy, M. Sun, O. Wallberg, C. Hulteberg and P. Tunå, Membrane Separation of the Base-Catalyzed Depolymerization of Black Liquor Retentate for Low-Molecular-Mass Compound Production, *Membranes*, 2019, **9**(8), 102.

49 H. Werhan, A. Farshori and P. R. von Rohr, Separation of lignin oxidation products by organic solvent nanofiltration, *J. Membr. Sci.*, 2012, **423**, 404–412.
50 T. G. Rials and W. G. Glasser, *Engineering plastics from lignin-XIII. Effect of lignin structure on polyurethane network formation*, 1986.
51 W. G. Glasser, About making lignin great again—Some lessons from the past, *Front. Chem.*, 2019, **7**, 565.
52 M. Issaoui and L. Limousy, Low-cost ceramic membranes: Synthesis, classifications, and applications, *C. R. Chim.*, 2019, **22**, 175–187.
53 I. J. a. G. Galjaard, *Back to Ceramics*, Water Environment & Technology, 2020, (June), pp. 32–37.
54 R. W. Baker, Future directions of membrane gas separation technology, *Ind. Eng. Chem. Res.*, 2002, **41**(6), 1393–1411.
55 C. W. Johnson, D. Salvachúa, N. A. Rorrer, B. A. Black, D. R. Vardon, P. C. S. John, N. S. Cleveland, G. Dominick, J. R. Elmore, N. Grundl, P. Khanna, C. R. Martinez, W. E. Michener, D. J. Peterson, K. J. Ramirez, P. Singh, T. A. VanderWall, A. N. Wilson, X. Yi, M. J. Biddy, Y. J. Bomble, A. M. Guss and G. T. Beckham, Innovative chemicals and materials from bacterial aromatic catabolic pathways, *Joule*, 2019, **3**(6), 1523–1537.
56 A. Al-Karaghouli and L. L. Kazmerski, Energy consumption and water production cost of conventional and renewable-energy-powered desalination processes, *Renewable Sustainable Energy Rev.*, 2013, **24**, 343–356.
57 R. E. Davis, N. J. Grundl, L. Tao, M. J. Biddy, E. C. Tan, G. T. Beckham, D. Humbird, D. N. Thompson and M. S. Roni, *Process design and economics for the conversion of Lignocellulosic biomass to hydrocarbon fuels and coproducts: 2018 biochemical design case update; Biochemical deconstruction and conversion of biomass to fuels and products via integrated biorefinery pathways*, National Renewable Energy Lab.(NREL), Golden, CO (United States), 2018.
58 V. S. Thompson, J. A. Lacey, D. Hartley, M. A. Jindra, J. E. Aston and D. N. Thompson, Application of air classification and formulation to manage feedstock cost, quality and availability for bioenergy, *Fuel*, 2016, **180**, 497–505.
59 G. Rudolph, B. Al-Rudainy, J. Thuvander and A.-S. Jönsson, Comprehensive Analysis of Foulants in an Ultrafiltration Membrane Used for the Treatment of Bleach Plant Effluent in a Sulfite Pulp Mill, *Membranes*, 2021, **11**(3), 201.
60 D. Salvachúa, A. Z. Werner, I. Pardo, M. Michalska, B. A. Black, B. S. Donohoe, S. J. Haugen, R. Katahira, S. Notonier and K. J. Ramirez, Outer membrane vesicles catabolize lignin-derived aromatic compounds in Pseudomonas putida KT2440, *Proc. Natl. Acad. Sci. U. S. A.*, 2020, **117**(17), 9302–9310.
61 C. Del Cerro, E. Erickson, T. Dong, A. R. Wong, E. K. Eder, S. O. Purvine, H. D. Mitchell, K. K. Weitz, L. M. Markillie and M. C. Burnet, Intracellular pathways for lignin catabolism in white-rot fungi, *Proc. Natl. Acad. Sci. U. S. A.*, 2021, **118**(9), 1–10.
62 A. Sluiter, B. Hames, R. Ruiz, C. Scarlata, J. Sluiter, D. Templeton and D. Crocker, *Determination of structural carbohydrates and lignin in biomass*, Laboratory analytical procedure, 2008, vol. 1617(1), pp. 1–16.